Tunneling magnetoresistance anomalies in a Coulomb blockaded quantum dot

Piotr Stefański*

Institute of Molecular Physics, Polish Academy of Sciences, ul. Smoluchowskiego 17, 60-179 Poznań, Poland

(Received 5 December 2008; revised manuscript received 15 January 2009; published 17 February 2009)

We consider quantum transport and tunneling magnetoresistance (TMR) through an interacting quantum dot in the Coulomb blockade regime, attached to ferromagnetic leads. We show that there exist two kinds of anomalies of TMR, which have different origins. One type, associated with the TMR sign change and appearing at conductance resonances, is of a single-particle origin. The second type, inducing a pronounced increase in TMR value far beyond 100%, is caused by electron correlations. It is manifested in between Coulomb blockade conductance peaks. Both types of anomalies are discussed for zero and finite biases, and their robustness to the temperature increase is also demonstrated. The results are presented in the context of recent experiments on semiconductor quantum dots in which similar features of TMR have been observed.

DOI: 10.1103/PhysRevB.79.085312 PACS number(s): 85.75.−d, 73.23.Hk, 73.63.−b

I. INTRODUCTION

Spin dependent tunneling phenomena have attracted much scientific attention recently mostly due to the promising potential applications for magnetic sensors and magnetic random access memories. Early work of Moodera *et al.*,[1] showing large reproducible tunneling magnetoresistance (TMR) effect of ferromagnetic tunnel junctions with Al_2O_3 spacer measured at room temperature, was one of the first steps initiating an avalanche of both theoretical and experimental investigations. The results were well understood within Julliere's model.[2] Within this model the TMR effect is described in terms of the density-of-states polarizations at Fermi energy of left (L) and right (R) ferromagnetic electrodes: $\mathrm{TMR}=2\mathrm{P}_L\mathrm{P}_R/(1-\mathrm{P}_L\mathrm{P}_R)$. The electronic structure of the spacer is assumed to be featureless. It appeared that this model was too simple to understand the experimental results that further arose. The interface resonant states appearing as a result of energy structure mismatch of the ferromagnetic lead and insulating spacer have considerable influence on the TMR value.[3,4] In particular, symmetry of these states can select spin-polarized bands in ferromagnetic electrode and enhance tunneling through the insulating barrier. Moreover, a modification of the energy structure of the spacer and its bonding to the ferromagnetic leads can switch the polarization of the current and also change the sign of tunneling magnetoresistance. These features can be controlled by a proper modification of the spacer composition.[3] It was also shown that the defect states, present in the insulating spacer separating two ferromagnetic leads, can dramatically change the exchange interaction between the leads[5] and affects TMR in the way not understood within Julliere's model. Recently it has also been derived that the scattering of electrons on nonmagnetic impurities present in the nanojunction barrier can cause the switching of TMR sign.[6]

In recent years, due to rapid development of nanotechnology, a new kind of "spacer" became available to be put between ferromagnetic leads. Importantly, the electronic properties of these spacers are well controllable. These are semiconductor quantum dots[7] (QDs). They have well defined discrete energy spectrum, whose position with respect to the chemical potential of the leads can easily be capacitatively tuned by electric field of a nearby gate. This in turn gives the possibility of electrical control of the TMR effect for such a device, which opens new possibilities of applications. Manipulation of the spin by electric field is one of the central issues of spintronics, which is regarded as a promising alternative for traditional charge-based electronics. Electron interactions inside the dots cause dramatic effects in their conductance, displaying quantum Coulomb blockade[8] and Kondo effect.[9] Recently TMR measurements have been performed for such designed devices: InAs quantum dots coupled to nickel or cobalt electrodes.[10–13] These experiments show a rich TMR behavior, including the changes in the TMR sign and appearance of its maximum far exceeding 100%. Spin transport and gate control of the tunneling magnetoresistance has also been realized in carbon nanotubes.[14,15] The variety of TMR anomalies observed in those systems is also ascribed to the discreetness of the nanotube energy structure.

Tunneling magnetoresistance oscillations caused by the classical Coulomb blockade at a small metallic droplet coupled to ferromagnetic electrodes had already been predicted long ago.[16] The TMR value can also change its sign due to strong electron correlations inside the dot in Kondo regime, as was shown theoretically.[17,18] It is a result of the current enhancement by the Kondo resonance when the dot is coupled to the leads of antiparallel (AP) spin configuration.

In the present paper we make an attempt to describe experimentally encountered anomalies of TMR (Refs. 10–12) for the InAs quantum dots in Coulomb blockade regime. We utilize the model of an interacting quantum dot with one level active in transport, coupled to ferromagnetic leads. We show that TMR sign switching is caused by the resonances of the dot level with one of the lead chemical potential in presence of the large asymmetry of the dot-lead coupling. We also predict that electron-electron interactions inside the dot have a decisive role in the formation of the TMR maximum, which exceeds 100 %. Recently, within the similar model device, we also introduced a proposal of the electrical control of the spin polarization of the current.[19] We will show that the correlation induced switching of the spin direction of the current is closely related to the TMR sign change at Coulomb blockade.

II. THEORETICAL APPROACH

The device is described by Anderson Hamiltonian,[20] where the dot takes the role of magnetic impurity and the (polarized) leads are analogs of host metal:

$$H = \epsilon_d d_\sigma^+ d_\sigma + U n_\sigma n_{\bar{\sigma}} + \sum_{k,\sigma,\alpha=L,R} [t_\alpha c_{k\alpha,\sigma}^+ d_\sigma + \text{H.c.}] + \sum_{k,\sigma,\alpha=L,R} \epsilon_{k\alpha,\sigma} c_{k\alpha,\sigma}^+ c_{k\alpha,\sigma}. \tag{1}$$

The first two terms describe the dot with the presence of Coulomb interactions U. The bare dot level is shifted by the gate voltage acting on the dot capacitatively: $\epsilon_d \equiv \epsilon_d - V_g$, and its initial position for $V_g=0$ is assumed to coincide with Fermi level $\epsilon_d = \epsilon_F = 0$. The third term describes the tunneling between the dot and the leads, represented by the last term in Eq. (1). The electron energy in the leads is spin dependent, $\sigma=\uparrow,\downarrow$, because the leads are assumed to be spin polarized. We neglect the spin dependence of the tunneling matrix elements $t_\alpha(\alpha=L,R)$ which are rather dependent on the potential barrier between the dot and a given lead. Thus, the spin dependence of the QD level width $(\Gamma_\sigma/2)=(1/2)\Sigma_\alpha\Gamma_{\alpha\sigma}$; $\Gamma_{\alpha\sigma}=2\pi|t_\alpha|^2\rho_{\alpha\sigma}$ is caused by the coupling to the leads with different spectral densities $\rho_{\alpha\uparrow}\neq\rho_{\alpha\downarrow}$, which are assumed to be featureless and constant.

Let us define the polarization of the quantity X, $\mathrm{P}_X=(X_\uparrow - X_\downarrow)/(X_\uparrow + X_\downarrow)$. For the lead α it is: $\mathrm{P}_\alpha=(\rho_{\alpha\uparrow}-\rho_{\alpha\downarrow})/(\rho_{\alpha\uparrow}+\rho_{\alpha\downarrow})$, which can be expressed by the spin-dependent QD widths:

$$\mathrm{P}_\alpha = (\Gamma_{\alpha\uparrow} - \Gamma_{\alpha\downarrow})/(\Gamma_{\alpha\uparrow} + \Gamma_{\alpha\downarrow}). \tag{2}$$

To calculate TMR we will consider parallel (P), $\mathrm{P}_R=\mathrm{P}_L$, and AP, $\mathrm{P}_R=-\mathrm{P}_L$, lead polarization arrangements. The asymmetry of the dot-lead coupling is described by α parameter. Because of validity of Eq. (2), the relations between dot level width components from left and right leads follow for P and AP configurations:

$$\Gamma_{R\sigma}^{\mathrm{P}} = \alpha\Gamma_{L\sigma}^{\mathrm{P}}, \quad \Gamma_{R\sigma}^{\mathrm{AP}} = \alpha\Gamma_{L\bar{\sigma}}^{\mathrm{AP}}, \quad \sigma,\bar{\sigma}=\uparrow,\downarrow. \tag{3}$$

Tunneling magnetoresistance is calculated from the formula: $\mathrm{TMR}=(\mathcal{G}^{\mathrm{P}}-\mathcal{G}^{\mathrm{AP}})/\mathcal{G}^{\mathrm{AP}}$, where $\mathcal{G}$ are appropriate conductances calculated for parallel and antiparallel configurations.

The retarded dot Green's function $G_\sigma^r(t-t')=-i\theta(t-t')\langle d_\sigma(t)d_\sigma^\dagger(t')+d_\sigma^\dagger(t')d_\sigma(t)\rangle$ is obtained by solving the set of equations of motion of the Green's functions in the Hubbard I approximation.[21] Within this approximation the two-particle Green's functions describing spin-flip processes (generating Kondo effect) on the localized level are neglected. The Green's functions that describe the normal scattering of band electrons on an impurity are approximated by decoupling of band electrons from impurity electrons. The Hubbard approximation is valid for large U/Γ ratio, when the Hubbard subbands are well separated in energy scale. For numerical calculations we assumed $\Gamma_{L\uparrow}=0.3U$, in which the other width components are calculated from Eqs. (2) and (3) for given lead polarization and asymmetry α.

The Hubbard approximation is the simplest scheme which describes correlated electrons, placed on the approximation scale between Hartree-Fock approximation for interacting but uncorrelated electrons, and the schemes for strongly correlated electrons, leading to Kondo physics. Thus, it is most suitable for the description of a spin-degenerate QD level in the Coulomb blockade regime of the lead-dot coupling, the limit realized in recent experiments.[10–12]

The Fourier-transformed expression for QD Green's function with the spin $\sigma=\uparrow,\downarrow$ for given β=P or AP arrangement has the form:

$$G_\sigma^{r,\beta}(\omega) = \left[\frac{\omega-\epsilon_d}{1+\dfrac{\langle n_{\bar{\sigma}}\rangle^\beta U}{\omega-\epsilon_d-U}} + \frac{i\Gamma_\sigma^\beta}{2}\right]^{-1} \simeq \frac{1-\langle n_{\bar{\sigma}}\rangle^\beta}{\omega-\epsilon_d+\dfrac{i\Gamma_\sigma^\beta}{2}} + \frac{\langle n_{\bar{\sigma}}\rangle^\beta}{\omega-\epsilon_d-U+\dfrac{i\Gamma_\sigma^\beta}{2}}. \tag{4}$$

Equation (4) has been written as the sum of two Hubbard resonances, $\epsilon_d^{\mathrm{I}}=\epsilon_d$ and $\epsilon_d^{\mathrm{II}}=\epsilon_d+U$, whose spectral weights are controlled by the dot level occupancy with the opposite spin $\bar{\sigma}$. This feature directly reflects Coulomb interactions between electrons with opposite spins.

The spin components of the dot occupancy have been calculated self-consistently from the set of coupled equations:

$$\langle n_\sigma\rangle^\beta = -\frac{i}{2\pi}\int G_\sigma^{<,\beta}(\omega,\langle n_{\bar{\sigma}}\rangle^\beta)d\omega,$$

$$\langle n_{\bar{\sigma}}\rangle^\beta = -\frac{i}{2\pi}\int G_{\bar{\sigma}}^{<,\beta}(\omega,\langle n_\sigma\rangle^\beta)d\omega. \tag{5}$$

The "lesser" dot Green's function $G^{<,\beta}$ can be expressed by the spectral density of the dot,[22] $\rho_\sigma^\beta(\omega)=-(1/\pi)\Im G_\sigma^{r,\beta}(\omega)$, $G_\sigma^{<,\beta}(\omega)=2i\pi\bar{f}(\omega)\rho_\sigma^\beta(\omega)$. Nonequilibrium distribution function $\bar{f}=[\Gamma_{L\sigma}^\beta f_L+\Gamma_{R\sigma}^\beta f_R]/(\Gamma_{L\sigma}^\beta+\Gamma_{R\sigma}^\beta)$ has a two-step profile defined by the chemical potential in the leads: $f_{L/R}\equiv f(\omega\mp eV)$, and collapses into equilibrium Fermi-Dirac distribution function $f\equiv f_L=f_R$ in the limit of zero bias between the leads, $eV\to 0$. The current is calculated within Landauer formalism from the relation:[22]

$$J^\beta = \frac{e}{2\hbar}\sum_\sigma \int d\omega[f_L-f_R]\frac{\Gamma_{L\sigma}^\beta\Gamma_{R\sigma}^\beta}{\Gamma_{L\sigma}^\beta+\Gamma_{R\sigma}^\beta}\rho_\sigma^\beta(\omega). \tag{6}$$

In the limit of zero bias the conductance has the form:

$$\mathcal{G}^\beta = \frac{\partial J^\beta}{\partial V} = \frac{e^2}{\hbar}\sum_\sigma \int d\omega\left(-\frac{\partial f}{\partial\omega}\right)\frac{\Gamma_{L\sigma}^\beta\Gamma_{R\sigma}^\beta}{\Gamma_{L\sigma}^\beta+\Gamma_{R\sigma}^\beta}\rho_\sigma^\beta(\omega). \tag{7}$$

III. BEHAVIOR OF THE SYSTEM AT ZERO BIAS

For all numerical results presented we have chosen the left lead polarization $\mathrm{P}_L=0.5$ and temperature $T=0.01U$. This range is typical for experiments;[10–12] it gives the temperature of 174 mK for $U=15$ meV.[11]

In Fig. 1 calculated TMR evolution with the change in gate voltage for different α asymmetry parameter is demon-

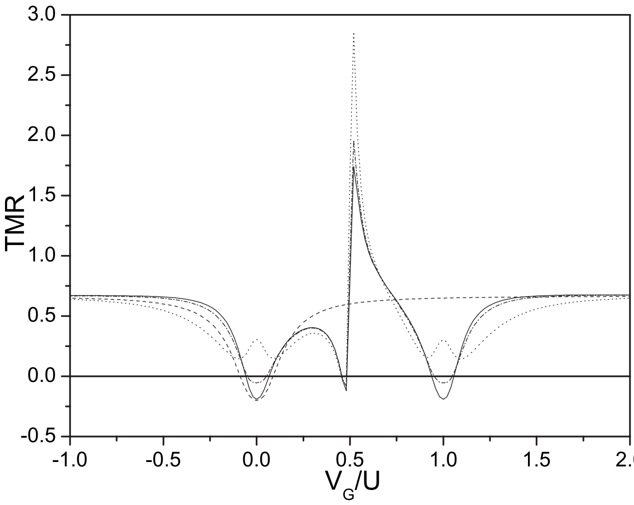

FIG. 1. TMR dependence on gate voltage calculated for $T=0.01U$, $P_L=0.5$, and zero bias for various asymmetry parameters: $\alpha=0.1$—solid, $\alpha=1$—dotted, and $\alpha=0.2$—dash-dotted curves. The dashed line is for noninteracting dot and $\alpha=0.1$.

strated. In order to understand various TMR anomalies shown in Fig. 1, it is instructive to analyze analytically TMR expression at $T=0$. The conductance for a given spin and lead configuration β has the following form in this limit:

$$\mathcal{G}_\sigma^\beta = \frac{e^2}{h}\frac{\Gamma_{L\sigma}^\beta\Gamma_{R\sigma}^\beta}{\left[\dfrac{\epsilon_d(\epsilon_d+U)}{\epsilon_d+U(1-\langle n_{\bar{\sigma}}\rangle^\beta)}\right]^2+\dfrac{1}{4}(\Gamma_{L\sigma}^\beta+\Gamma_{R\sigma}^\beta)^2}. \tag{8}$$

Consider the situation when ϵ_d^{I} or ϵ_d^{II} Hubbard level crosses Fermi level (at $V_g=0$ or $V_g=U$). In this case Eq. (8) takes the form:

$$\mathcal{G}_\sigma^\beta = \frac{e^2}{h}\frac{\Gamma_{L\sigma}^\beta\Gamma_{R\sigma}^\beta}{\dfrac{1}{4}(\Gamma_{L\sigma}^\beta+\Gamma_{R\sigma}^\beta)^2}. \tag{9}$$

The conductance has exactly the same form as for noninteracting dot level of Green's function: $\mathcal{G}_\sigma^r=[\omega-\epsilon_d+i(\Gamma_\sigma^\beta/2)]^{-1}$ crossing Fermi level, $\epsilon_d=\epsilon_F$. Thus, these TMR features are of the single-particle origin and can be described in the limit of noninteracting electrons. In Fig. 1 also the TMR curve for noninteracting dot level, calculated for $\alpha=0.1$, is shown. The minimum at $V_g=0$ coincides with one of interacting case for first Hubbard level in resonance with Fermi level $\epsilon_d^{\mathrm{I}}=\epsilon_F$.

Taking into account the relations between the level widths [Eq. (3)], it can be shown by straightforward calculation that, for $\epsilon_d^{\mathrm{I}}=0$ or $\epsilon_d^{\mathrm{II}}=0$, the spin components of conductance for parallel and antiparallel configurations are (in units of e^2/h):

$$\mathcal{G}_\uparrow^{\mathrm{P}} = \mathcal{G}_\downarrow^{\mathrm{P}} = \frac{4\alpha}{(1+\alpha)^2}, \tag{10}$$

and

$$\mathcal{G}_{\uparrow/\downarrow}^{\mathrm{AP}} = -\frac{4\alpha(\mathrm{P}_L^2-1)}{[\mathrm{P}_L(1-\alpha)\pm(1+\alpha)]^2}, \tag{11}$$

where also the relation between spin-dependent widths from Eq. (2): $\Gamma_{L\downarrow}=-\Gamma_{L\uparrow}(\mathrm{P}_L-1)/(\mathrm{P}_L+1)$, has been applied.

For symmetric coupling ($\alpha=1$), the conductance for parallel configuration $\mathcal{G}^{\mathrm{P}}=\mathcal{G}_\uparrow^{\mathrm{P}}+\mathcal{G}_\downarrow^{\mathrm{P}}$ reaches its maximum value of $2e^2/h$. It is reflected in the TMR curve in Fig. 1, which also displays a local maximum at the conductance resonances at $V_g=0$ and $V_g=U$. The conductances for antiparallel configuration and $\alpha=1$ are $\mathcal{G}_\uparrow^{\mathrm{AP}}=\mathcal{G}_\downarrow^{\mathrm{AP}}=-(\mathrm{P}_L^2-1)$, which yields $\mathrm{TMR}=\mathrm{P}_L^2/(1-\mathrm{P}_L^2)>0$. Thus, for symmetric dot-lead coupling, the TMR has positive sign at the conductance resonances. The situation changes for asymmetric coupling, $\alpha<1$. In this case TMR at resonances takes the form:

$$\mathrm{TMR} = \frac{-[\mathrm{P}_L^2(1-\alpha)^2-(1+\alpha)^2]^2}{(1+\alpha)^2(\mathrm{P}_L^2-1)[\mathrm{P}_L^2(1-\alpha)^2+(1+\alpha)^2]}-1, \tag{12}$$

and for $\alpha\ll 1$, it changes the sign to negative: $\mathrm{TMR}=-2\mathrm{P}_L^2/(\mathrm{P}_L^2+1)<0$, as shown in Fig. 1.

Let us summarize the above discussed single-particle TMR sign changes within a simple physical picture. For the perfect symmetric coupling, $\alpha=1$, the transmission through the dot in parallel configuration reaches the conductance quantum in both spin channels, $\mathcal{G}_\uparrow^{\mathrm{P}}=\mathcal{G}_\downarrow^{\mathrm{P}}=e^2/h$. This is caused by the perfect matching of the spectral densities of spin up and spin down of the left lead to the corresponding spectral densities of the right lead at the Fermi level. It also results that the spin-dependent level widths due to the coupling to the left lead and to the right lead are equal [see Eq. (3)]. In antiparallel configuration and $\alpha=1$, this is not the case; the number of states of spin up and spin down in the left lead at the Fermi level are different as compared to the right lead and also the corresponding level widths are not equal. Thus, the conductance in antiparallel configuration is less than conductance quantum, $\mathcal{G}_\uparrow^{\mathrm{AP}}=\mathcal{G}_\downarrow^{\mathrm{AP}}=(3/4)(e^2/h)$ for $\mathrm{P}_L=0.5$ and $\mathrm{TMR}>0$. Note that, for unpolarized leads, $\mathrm{P}_L=0$, the matching of the spectral densities is retained, and the conductances $\mathcal{G}_\uparrow^{\mathrm{AP}}=\mathcal{G}_\downarrow^{\mathrm{AP}}=e^2/h$ reach conductance quantum. When the asymmetry of the dot-lead coupling is increased, $\alpha<1$, the tunneling between the dot and the right lead is reduced, which destroys the perfect matching of the widths in P configuration: $\Gamma_{R\uparrow}^{\mathrm{P}}\neq\Gamma_{L\uparrow}^{\mathrm{P}}$ and $\Gamma_{R\downarrow}^{\mathrm{P}}\neq\Gamma_{L\downarrow}^{\mathrm{P}}$. It results in a gradual decrease in both spin conductance components in P configuration with the increase in α. More interesting situation takes place in AP configuration. The $\mathcal{G}_\uparrow^{\mathrm{AP}}$ conductance component, which describes the tunneling of spin-up excess electrons ($\mathrm{P}_L>0$) from the left lead via resonant dot state into minority up-spin subband of the right lead ($\mathrm{P}_R<0$) decreases with the increase in the coupling asymmetry because the width $\Gamma_{R\uparrow}^{\mathrm{AP}}$ which is less than $\Gamma_{L\uparrow}^{\mathrm{AP}}$ even for $\alpha=1$ is further decreased by lowering α. It increases the mismatch between the widths in this spin sector. Different relation is encountered between the widths in the AP spin-down channel. Initially, for $\alpha=1$ we have $\Gamma_{R\downarrow}^{\mathrm{AP}}>\Gamma_{L\downarrow}^{\mathrm{AP}}$ and, by the decrease in α, the value of $\Gamma_{R\downarrow}^{\mathrm{AP}}$ is lowered. When it reaches the value $\Gamma_{R\downarrow}^{\mathrm{AP}}=\Gamma_{L\downarrow}^{\mathrm{AP}}$, we have a perfect symmetric coupling in this channel. Thus, the *de-*

crease in the dot-lead coupling symmetry causes an *increase* in the coupling symmetry in the spin-down sector when the system in AP configuration. The component $\mathcal{G}_{\downarrow}^{\mathrm{AP}}$ increases and starts to dominate over other conductance components causing TMR<0 for small α. It can be checked from Eq. (11) that $\mathcal{G}_{\downarrow}^{\mathrm{AP}}$ reaches full transmission limit for $\alpha=1/3$ when $\mathrm{P}_L=0.5$. This enhancement of one of the conductance spin components in AP configuration can easily be generalized to other AP arrangements. For instance, if the polarization of the left lead were assumed to be negative, the $\mathcal{G}_{\uparrow}^{\mathrm{AP}}$ would be enhanced by the decrease in α.

Similarly, as discussed, TMR sign changes have been observed in quantum dots[11,12] and in carbon nanotubes[14] coupled to ferromagnetic electrodes. They are also interpreted in terms of the asymmetry of the coupling to the leads.

Consider now the region in which the dot is in Coulomb blockade. In this case for $\epsilon_d=-U/2$ exactly one electron is present at the dot $\langle n_{\uparrow}\rangle^{\beta}+\langle n_{\downarrow}\rangle^{\beta}=1$. There are considerable TMR anomalies near this point (see Fig. 1); TMR can change its sign or can be greatly enhanced to exceed 100%. These anomalies are caused by electron-electron interactions. The peculiar behavior of TMR in this region is caused by interplay of the two factors. The first is caused by the coupling (and its asymmetry) of the dot to the spin-polarized leads. It determines the widths of the conductance peaks for parallel and antiparallel configurations. The second factor is electron correlations which are the strongest in this region.[23] They cause the spin components of the occupancies to be close to one-half at Coulomb blockade. The TMR anomalies here can be understood by analyzing the spin components of the conductance for given lead polarization arrangement [Eq. (8)]. For $\epsilon_d\sim-U/2$ and $\langle n_{\bar{\sigma}}\rangle^{\beta}\sim0.5$, the denominator $\epsilon_d+U(1-\langle n_{\bar{\sigma}}\rangle)$ is very small, causing $\mathcal{G}_{\sigma}^{\beta}$ to be small. Depending on the lead polarizations and the strength of the Coulomb interactions, the components of the conductances defining TMR get their minimal values for different positions of the dot level. The same mechanism causes sudden current polarization switching in the region of $\epsilon_d\sim-U/2$ as discussed in Ref. 19. Indeed, it is shown in Fig. 2 that for P and AP configurations the value of conductance polarization $\mathrm{P}_{\mathcal{G}}^{\beta}$ performs a rapid oscillation and additionally it changes sign for AP configuration.

TMR value in this region is very sensitive to the change in the conductance in AP configuration. Consider first the perfect symmetric coupling, $\alpha=1$. For $\mathrm{P}_R=-\mathrm{P}_L$ the total widths of the dot level are equal $\Gamma_{\uparrow}=\Gamma_{\downarrow}$ because of relation $\Gamma_{L\uparrow}=\Gamma_{R\downarrow}$ and $\Gamma_{L\downarrow}=\Gamma_{R\uparrow}$ [Eq. (3)]. Thus, in the symmetric AP arrangement, the dot behaves as if it were coupled to unpolarized leads. In such a case spin components of the conductance are equal, $\mathcal{G}_{\uparrow}^{\mathrm{AP}}=\mathcal{G}_{\downarrow}^{\mathrm{AP}}$, in the whole range of gate voltages and also the occupancies $\langle n_{\uparrow}\rangle^{\mathrm{AP}}=\langle n_{\downarrow}\rangle^{\mathrm{AP}}$ are equal. The QD occupancy curve displays a plateau at $\langle n_{\uparrow}\rangle=\langle n_{\downarrow}\rangle\sim0.5$ due to Coulomb blockade.[19] Moreover, for particle-hole symmetric case, $\epsilon_d=-U/2$, the occupancies are $\langle n_{\uparrow}\rangle^{\mathrm{AP}}=\langle n_{\downarrow}\rangle^{\mathrm{AP}}=0.5$, giving $\mathcal{G}_{\uparrow}^{\mathrm{AP}}=\mathcal{G}_{\downarrow}^{\mathrm{AP}}=0$. This feature causes an infinite TMR value for $\alpha=1$ at $T=0$. For asymmetric coupling, $\alpha<1$, and finite temperature, the relation $\mathcal{G}_{\uparrow}^{\mathrm{AP}}=\mathcal{G}_{\downarrow}^{\mathrm{AP}}$ is still fulfilled at the gate voltage of TMR maximum but the conductances have small finite value. From the condition of

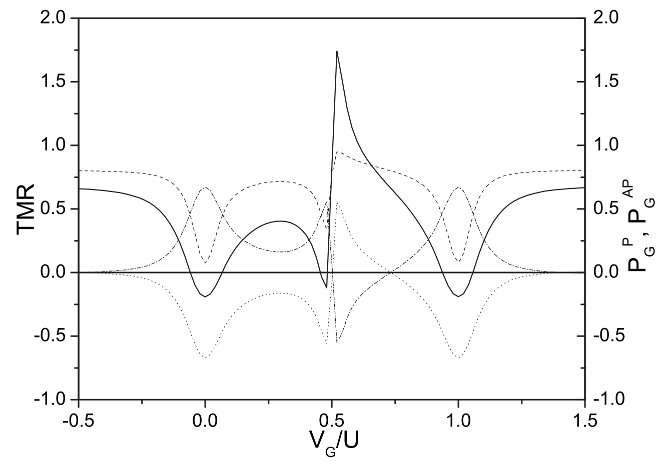

FIG. 2. TMR (solid curve) vs gate voltage calculated for $\alpha=0.1$ at $T=0.01U$ and zero bias. The corresponding conductance polarizations $\mathrm{P}_{\mathcal{G}}^{\mathrm{P}}$ (dashed curve) and $\mathrm{P}_{\mathcal{G}}^{\mathrm{AP}}$ (dotted curve) are also shown. Dash-dotted curve is for $-\mathrm{P}_{\mathcal{G}}^{\mathrm{AP}}$.

$\mathcal{G}_{\uparrow}^{\mathrm{AP}}=\mathcal{G}_{\downarrow}^{\mathrm{AP}}$ follows also the equality $\langle n_{\uparrow}\rangle^{\mathrm{AP}}=\langle n_{\downarrow}\rangle^{\mathrm{AP}}$ at gate voltage of TMR maximum, independently on α. It can easily be derived utilizing Eq. (8). At Coulomb blockade, the first term in the denominator is much larger than the second one and the relation [Eq. (3)] for AP configuration have to be used. Thus, at TMR maximum the conductance in AP configuration is unpolarized (the conductance polarization $\mathrm{P}_{\mathcal{G}}^{\mathrm{AP}}=0$ as shown in Fig. 2) and also the dot occupancy polarization is zero.

Strong enhancement of TMR at classical Coulomb blockade has also been predicted for ferromagnetic double tunnel junctions[24] as a result of cotunneling of electrons through metallic island. It has also been observed experimentally.[25,26] Our result provides an explanation of corresponding TMR maximum at quantum Coulomb blockade for semiconductor quantum dot. It is in relation with the recent TMR measurements for InAs quantum dot coupled to the Ni leads,[12] where the TMR enhancement above 300% has been observed at Coulomb blockade.

At the gate voltages for which TMR$=0$, following equalities apply $\mathcal{G}_{\uparrow}^{\mathrm{AP}}=\mathcal{G}_{\downarrow}^{\mathrm{P}}$ and $\mathcal{G}_{\downarrow}^{\mathrm{AP}}=\mathcal{G}_{\uparrow}^{\mathrm{P}}$. It implies that the conductance spin polarizations are opposite for parallel and antiparallel configurations: $\mathrm{P}_{\mathcal{G}}^{\mathrm{P}}=-\mathrm{P}_{\mathcal{G}}^{\mathrm{AP}}$ (compare corresponding curves in Fig. 2).

Let us now discuss the TMR sign change encountered at Coulomb blockade. It is shown in Fig. 2 that this TMR minimum coincides with the sharp minima of conductance polarizations; moreover $\mathrm{P}_{\mathcal{G}}^{\mathrm{AP}}<0$ here. The TMR minimum is caused by sharp polarization switching of the conductance in AP configuration. It is in contrast to P configuration, for which the conductance polarization does not change its sign. In P configuration the dot is coupled to the leads both having excess of electrons of the same spin (in our case spin up), and conductance of this spin dominates in the whole range of gate voltages, $\mathrm{P}_{\mathcal{G}}^{\mathrm{P}}>0$ (Fig. 2). In AP configuration, on the average, there is no such excess of electrons of particular spin coming from the leads. Thus, $\mathcal{G}_{\uparrow}^{\mathrm{AP}}$ and $\mathcal{G}_{\downarrow}^{\mathrm{AP}}$ are comparable in magnitude, and the interactions between spin-up and spin-down electrons cause more dramatic changes in the con-

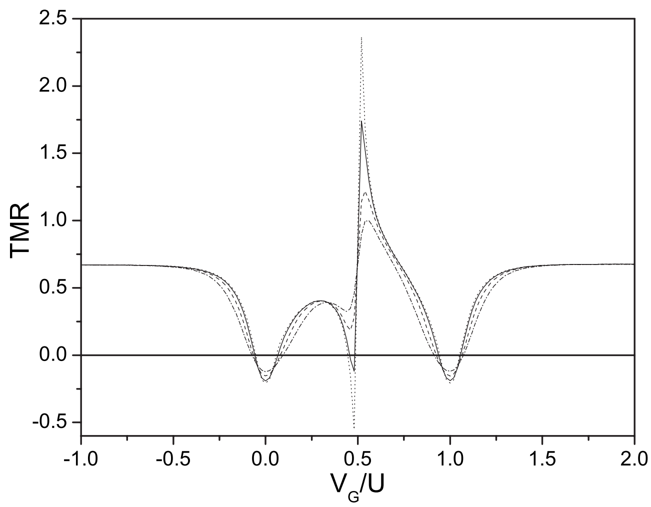

FIG. 3. Temperature dependence of the zero-bias TMR calculated for α=0.1 and P_L=0.5: T=0—dotted, T=0.01U—solid, T=0.02U—dashed, and T=0.03U—dash-dotted curves.

ductance polarization. Apart from electron-electron interactions, which cause the conductance polarization switching in AP configuration, the mechanism of enhancement of the conductance component $\mathcal{G}_{\downarrow}^{AP}$ for small α works also here, similarly as discussed for single-particle origin TMR sign change. The transmission in the spin-down channel of AP configuration dominates here over other conductance components and causes TMR<0. There is no unique condition for negative TMR minimum to appear at Coulomb blockade and it depends on the value of initial lead polarization. For higher P_α, the conductance in P configuration will dominate ($P_{\mathcal{G}}^{P}$ curve then is shifted upward) and TMR will not change sign in spite of conductance polarization switching in AP configuration (not shown). The polarization $P_{\mathcal{G}}^{AP}$ behaves similarly as in the case of configuration with one lead polarized.[19] The TMR sign change here also fades out rapidly with increase in temperature [Fig. 3] because the $P_{\mathcal{G}}^{AP}$ is very sensitive to the temperature change in this region. At higher temperatures $P_{\mathcal{G}}^{AP}$ switching decays quickly. This sensitivity in the region of $V_g \sim U/2$ has been shown in Ref. 19 for one of the leads polarized.

It could be counterintuitive that the conductance polarization $P_{\mathcal{G}}^{P}$ reaches values larger than the leads polarizations P_α=0.5 for $|V_g| \ll \epsilon_F$, as displayed in Fig. 2. We demonstrate that it is the case. In this limit the dot level is placed far from Fermi level; thus the dot is either unoccupied or fully occupied. Consider the unoccupied dot for configuration β, which is realized for large negative gate voltage. Inserting $\langle n_{\bar{\sigma}}\rangle^{\beta}$ =0 into Eq. (8) and noting that $(\epsilon_d)^2 \gg (\Gamma_\sigma/2)^2$, the conductance polarization can be written as

$$P_{\mathcal{G}}^{\beta} = \frac{\Gamma_{L\uparrow}^{\beta}\Gamma_{R\uparrow^{\beta}} - \Gamma_{L\downarrow}^{\beta}\Gamma_{R\downarrow}^{\beta}}{\Gamma_{L\uparrow}^{\beta}\Gamma_{R\uparrow}^{\beta} + \Gamma_{L\downarrow}^{\beta}\Gamma_{R\downarrow}^{\beta}}. \tag{13}$$

For β=P the relations of Eq. (3) are further utilized to give

$$P_{\mathcal{G}}^{P} = \frac{\Gamma_{L\uparrow}^2 - \Gamma_{L\downarrow}^2}{\Gamma_{L\uparrow}^2 + \Gamma_{L\downarrow}^2} = \frac{2P_L}{P_L^2 + 1}. \tag{14}$$

The last right-hand side expression has been obtained by substituting $\Gamma_{L\downarrow}$ calculated from Eq. (2). Note that the result is independent on α. Thus, for P_L=P_R=0.5 the conductance polarization $P_{\mathcal{G}}^{P}$=0.8. The same expression [Eq. (14)] is obtained for fully occupied dot $\langle n_{\bar{\sigma}}\rangle^{P}$=1 and noting that $(\epsilon_d + U)^2 \gg (\Gamma_\sigma/2)^2$. For antiparallel configuration, the conductance polarization $P_{\mathcal{G}}^{AP}$=0 in the limit of $|V_g| \ll \epsilon_F$, as shown in Fig. 2. It can straightforwardly be derived from Eq. (13) for β=AP when Eq. (3) is utilized. Note that TMR in the discussed limit of $|\epsilon_d| \ll \epsilon_F$ reaches value of 2/3 as predicted by Jullière's model[2] for two polarized leads separated by featureless tunnel barrier.

Temperature dependence of the TMR for asymmetric coupling α=0.1 is shown in Fig. 3. TMR anomalies in the regions of $V_g \sim 0$ and $V_g \sim U$ caused by the resonances of QD Hubbard levels ϵ_d^{I} and ϵ_d^{II} with the Fermi level are robust to the increase in temperature. The anomalies due to electron correlations situated in the range of Coulomb blockade $V_g \sim U/2$, in turn, are sensitive to these changes. It is caused by a temperature increase in the conductance spin components at the Coulomb blockade valley. However, the pronounced TMR maximum reaching 100% survives for T=0.03U [$\simeq$0.5 K for U=15 meV (Ref. 11)]. Contrarily, the negative TMR minimum rapidly disappears at higher temperature, as pointed out previously.

IV. BEHAVIOR OF THE SYSTEM AT FINITE BIAS

If the finite bias is applied to the system, an electron transport through excited states of the QD can be activated. In the Hubbard approximation, used for description of the device, these processes are not taken into account.

We consider two limits of the value of the bias applied as compared to the width of the QD level: small bias limit: $|eV| < \Gamma_\sigma$, and large bias limit when $|eV| > \Gamma_\sigma$. In the large bias limit the chemical potentials of the leads are well separated in energy scale. It implies also a good separation of the differential conductance resonance peaks which appear when any of the Hubbard QD levels crosses given chemical potential. Thus, the maxima and minima of TMR are also well separated. In the small bias limit the conductance resonances overlap each other which causes splitting of TMR minima and diminishing of TMR maximum at Coulomb blockade. In both the limits, a correspondence can be found between TMR features with those appearing at zero bias.

A. Small bias regime

The TMR behavior for eV=0.1U is shown in Fig. 4 for asymmetric coupling to the leads α=0.1 and temperature T=0.01U. One notices that the pronounced TMR minima present for V_g=0 and V_g=U are split when a finite bias is applied. For positive bias the left lead chemical potential μ_L is shifted upward by eV and right lead chemical potential μ_R is shifted downward by eV on energy scale. When gate voltage increases from negative values, it shifts the dot level from empty state regime toward Fermi bathes inside the leads. At first the ϵ_d^{I} level comes into resonance with μ_L and then with μ_R chemical potential. It causes the appearance of two peaks in conductance with the distance of doubled bias value between them (shown in Fig. 4) and consequently two

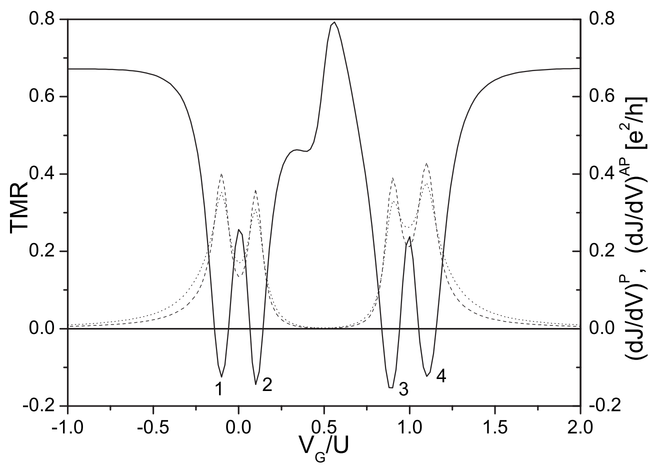

FIG. 4. TMR dependence on gate voltage (solid curve) for finite bias $eV=0.1U$ calculated at $T=0.01U$, $P_L=0.5$, and asymmetric coupling to the leads $\alpha=0.1$. The corresponding differential conductances $(\partial J/\partial V)^{P}$ (dotted curve) and $(\partial J/\partial V)^{AP}$ (dashed curve) are also shown.

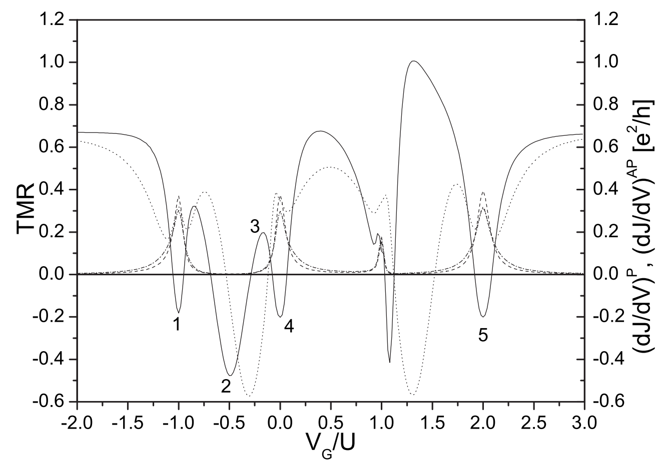

FIG. 5. TMR dependence on gate voltage (solid curve) for finite bias $eV=U$ calculated at $T=0.01U$, $P_L=0.5$, and asymmetric coupling to the leads $\alpha=0.1$. The corresponding differential conductances $(\partial J/\partial V)^{P}$ (dash-dotted curve) and $(\partial J/\partial V)^{AP}$ (dashed curve) are also shown. The dotted TMR curve is for symmetric coupling $\alpha=1$.

minima of TMR are produced, labeled by (1) and (2). Similarly, in the range of $V_g \sim U$ the second Hubbard level ϵ_d^{II} comes into resonance with μ_L and then with μ_R and minima (3) and (4) appear.

The maximum of TMR at $V_g \sim U/2$, distinct in case of zero bias, is diminished when the bias is finite. This maximum has been associated with the equality of $\mathcal{G}_{\uparrow}^{\mathrm{AP}}=\mathcal{G}_{\downarrow}^{\mathrm{AP}}$ and subsequently $\langle n_{\uparrow}\rangle^{\mathrm{AP}}=\langle n_{\downarrow}\rangle^{\mathrm{AP}}$ as discussed for $eV=0$. For finite bias this relation is still fulfilled. It can be checked by analyzing spin components of the differential conductance in Coulomb blockade region. However, the conductance for antiparallel configuration is enhanced by finite bias, and the splitting and shifting of the conductance peaks also appears. It causes a gradual diminishing of TMR maximum. The negative TMR minimum present for zero bias and associated with the rapid change in the conductance polarization $P_{\mathcal{G}}^{\mathrm{AP}}$ has disappeared at finite bias. It has been shown in Ref. 19 that this sudden conductance polarization switching also rapidly diminishes when finite bias is applied.

B. Large bias regime

Consider the case of $eV=U$ for which the left (right) chemical potential $\mu_L(\mu_R)$ is shifted upward (downward) by U on energy scale. The TMR vs gate voltage for such a bias and $\alpha=0.1$ is presented in Fig. 5 along with corresponding differential conductances.

Let us discuss various anomalies appearing in the TMR curve labeled by Arabic numbers. The TMR minima placed at the differential conductance resonances have single-particle origin. For instance, in point (1) at $V_g=-U$ the first Hubbard level ϵ_d^{I} coincides with μ_L and the second ϵ_d^{II} lying above is empty. At this point TMR has a (negative) minimum. This kind of minimum has appeared already for zero and small bias each time when the QD Hubbard level crossed chemical potential of the leads: for $eV=0$ it corresponds to the minimum at $V_g=0$ (see Fig. 1), and to the minimum (1) for small bias (Fig. 4). Similar correspondence is for minimum (5) at $V_g=2U$ where the second Hubbard level ϵ_d^{II} coincides with μ_R and ϵ_d^{I} is fully occupied. This minimum is analogous to the minimum at $V_g=U$ for zero bias and minimum (4) for small bias in Fig. 4. The minimum (4) at $V_g=0$ where ϵ_d^{II} in resonance with μ_L corresponds to the minimum (3) for small bias. One can also note series of maxima and minima appearing in between conductance resonances; for instance minimum (2) and maximum (3). These anomalies are caused by electron correlations and correspond to similar features of TMR at zero bias (Fig. 1) at $V_g \sim U/2$. For large bias, $eV \gg \Gamma_{\sigma}$, when the conductance resonances are well separated in energy scale, the Coulomb blockade TMR anomalies can be identified and their correspondence with zero-bias TMR features can also be established. In the small bias regime (Fig. 4), they are considerably diminished.

The TMR minima of single-particle origin, for instance, those numbered by (1), (4), and (5), transform into local maxima for symmetric dot-lead coupling, $\alpha=1$ (dotted curve). Similar feature was present for zero-bias case (Fig. 1). Thus, by experimentally tuning the coupling asymmetry one can resolve the mechanism causing a given TMR anomaly. Note that the TMR curve for $\alpha=1$ is symmetric with respect to $V_g=U/2$. At this point the Hubbard levels lay in the middle of the transport window of the width $2U$. For instance, when V_g is set to zero (to U), the $\epsilon_d^{\mathrm{II}}(\epsilon_d^{\mathrm{I}})$ comes into resonance with $\mu_L(\mu_R)$ and the other Hubbard level is shifted to the center of the transport window. It gives the same TMR feature for $\pm V_g$.

Consider now the bias dependence of TMR for the set gate voltage. In Fig. 6 the TMR bias dependencies for $\alpha=0.1$ and $\alpha=1$ calculated for $V_g=0$ are shown. Again, the TMR minima labeled by (1)–(3), present for large coupling asymmetry $\alpha=0.1$, can be identified as of single-particle origin. For minimum (2) at zero bias ϵ_d^{I} is in resonance with both μ_L and μ_R. For minimum (1) at $eV=-U$, the ϵ_d^{II} Hubbard level is in resonance with μ_L chemical potential, and for minimum (1) at $eV=U$, the ϵ_d^{II} Hubbard level is in resonance

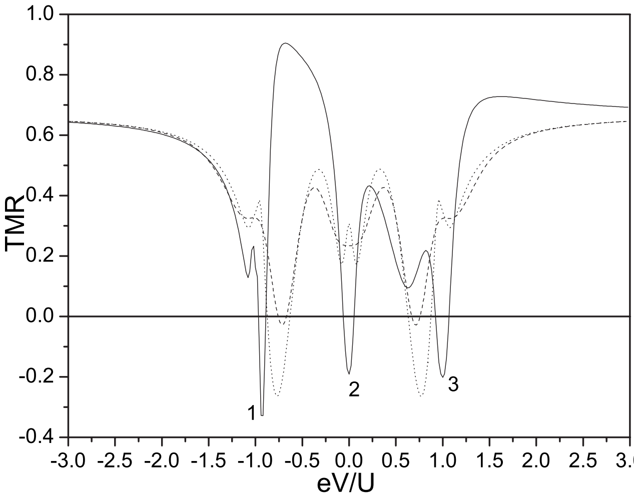

FIG. 6. TMR dependence on applied bias for the set gate voltage $V_g=0$ and $\mathrm{P}_L=0.5$, calculated at $T=0.01U$, and $\alpha=0.1$—solid curve, and $\alpha=1$—dotted curve; dashed curve—TMR for $\alpha=1$ and $T=0.06U$.

with μ_R chemical potential. These three minima disappear for symmetric coupling $\alpha=1$ and the local maxima develop instead as discussed before. The minima and maxima in the regions of $eV\sim\pm U/2$ correspond to electron correlations induced TMR anomalies discussed previously for zero bias (Fig. 1). These anomalies appear close to particle-hole symmetric case, when the Fermi level is situated in between dot Hubbard levels. In the present case, at $eV=-U/2$ the μ_L chemical potential is placed in between Hubbard levels in the sequence: $\mu_R<\epsilon_d^{\mathrm{I}}<\mu_L<\epsilon_d^{\mathrm{II}}$. At $eV=U/2$ the μ_R is in between Hubbard levels in sequence: $\mu_L<\epsilon_d^{\mathrm{I}}<\mu_R<\epsilon_d^{\mathrm{II}}$ in energy scale. From comparison of the TMR curves for $\alpha=1$ and $T=0.01U$, and at a higher temperature $T=0.06U$, one notes that the minima caused by electron correlations are much more sensitive to the temperature increase than maxima, similarly as in the case of zero bias (Fig. 3). Thus, by the increase in temperature one can distinguish the TMR minima of single-particle origin which are robust to the temperature change from those caused by electron interactions, sensitive to temperature.

For symmetric coupling to the leads, the TMR curve becomes symmetric with respect to $eV=0$. It is understood when one notices that the change in the bias direction is equivalent to the simultaneous exchange in $\mu_L\leftrightarrow\mu_R$ and $\epsilon_d^{\mathrm{I}}\leftrightarrow\epsilon_d^{\mathrm{II}}$. It gives for symmetric coupling, $\alpha=1$, the same value of TMR for $\pm eV$.

V. INFLUENCE OF EFFECTIVE MAGNETIC FIELDS

The dot attached to spin-polarized leads is influenced by two effective magnetic fields, which have different origin. (i) The hopping of electrons from the leads, which have an excess of one of the spin components, produces an occupancy polarization of the dot. Thus, the dot acquires magnetic moment $m_{\mathrm{QD}}^{\beta}=(\langle n_\uparrow\rangle^{\beta}-\langle n_\downarrow\rangle^{\beta})|\mu_s|$, where $\mu_s=g\mu_B s_z$ is the magnetic moment associated with spin-dependent (but degenerate) sublevels of ϵ_d and $s_z=\pm 1/2$. This effect can be regarded as if the dot were under influence of an external magnetic field and the Zeeman splitting of the dot energy level is produced. However, the value of the resultant dot's magnetic moment at given temperature is regulated by the relative position of the dot level with respect to the lead chemical potentials and electron-electron interactions. It has nonmonotonic behavior as shown in Fig. 7. It is in contrast to the usual Zeeman splitting of the level by external field H_{ext}, for which the magnetic moment $m=\tanh(|\mu_s|H_{\mathrm{ext}}/k_BT)$ increases monotonically with increase in the field. Let us discuss the general features of the dot magnetic moment for parallel and antiparallel configuration (Fig. 7). Because $\mathrm{P}_L>0$ the spin sublevels of each dot Hubbard level $\epsilon_{d\uparrow}^{\gamma}$ and $\epsilon_{d\downarrow}^{\gamma}(\gamma=\mathrm{I},\mathrm{II})$ have different widths $\Gamma_\uparrow>\Gamma_\downarrow$. For large, negative gate voltage ϵ_d^{II} is empty, and both the $\epsilon_{d\uparrow}^{\mathrm{I}}$ and $\epsilon_{d\downarrow}^{\mathrm{I}}$ are barely populated; the magnetic moment is small. The value of m_{QD} is positive because $\Gamma_\uparrow>\Gamma_\downarrow$ and $\epsilon_{d\uparrow}^{\mathrm{I}}$ is being populated earlier than $\epsilon_{d\downarrow}^{\mathrm{I}}$. When V_g increases, m_{QD} also increases, reaching the maximum. Further increase in V_g causes faster filling of $\epsilon_{d\downarrow}^{\mathrm{I}}$ sublevel because it is sharper than $\epsilon_{d\uparrow}^{\mathrm{I}}$. Thus, m_{QD} decreases toward zero at $V_g=0$, where $\epsilon_\sigma^{\mathrm{I}}$ is in resonance with Fermi energy ϵ_F. Further shift of $\epsilon_\sigma^{\mathrm{I}}$ causes further increase in $\langle n_\downarrow\rangle$ until a minimum of m_{QD} is reached. Note that the sequence of the filling of the first Hubbard level $\epsilon_\sigma^{\mathrm{I}}$, caused by inequality of the $\Gamma_\uparrow$ and $\Gamma_\downarrow$, is additionally enhanced by electron-electron interactions, manifested by the spectral weight dependence $\sim(1-\langle n_{\bar\sigma}\rangle)$ of $\epsilon_\sigma^{\mathrm{I}}$ [Eq. (4)]. After

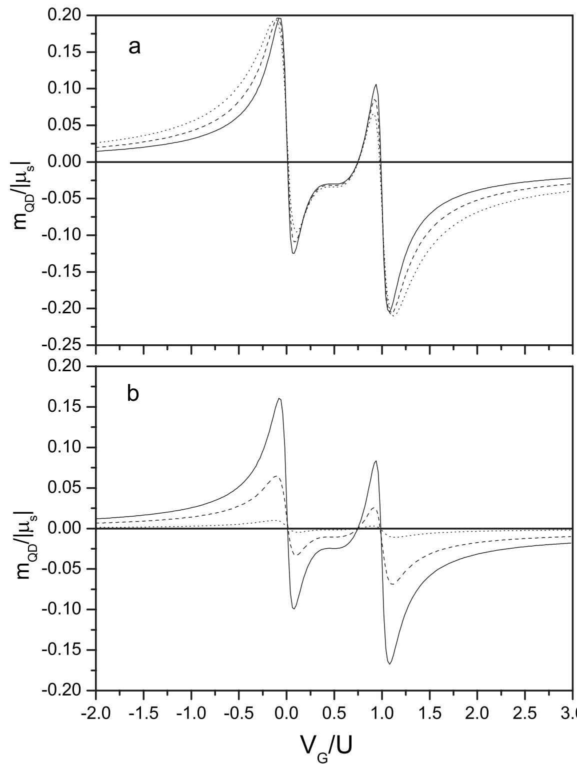

FIG. 7. Dot magnetic moment vs gate voltage for (a) parallel and (b) antiparallel configurations for various asymmetry α. Panels (a) and (b): $\alpha=0.1$—solid line, $\alpha=0.5$—dashed. Dotted line in panel (a) for $\alpha=1$ and in panel (b) for $\alpha=0.9$ ($m_{\mathrm{QD}}=0$ for $\alpha=1$ in antiparallel configuration). Calculated for zero bias at $T=0.01U$ and $\mathrm{P}_L=0.5$.

reaching $m_{\rm QD}$ minimum, the second Hubbard level $\epsilon_\sigma^{\rm II}$ starts to be filled and $m_{\rm QD}$ increases toward zero due to the same mechanism ($\Gamma_\uparrow > \Gamma_\downarrow$) as in the region of $V_g \sim 0$. The $m_{\rm QD} = 0$ at Coulomb blockade corresponds to the particle-hole symmetry case of $\epsilon_d = -U/2$ and $\langle n_\uparrow \rangle = \langle n_\downarrow \rangle = 0.5$ for unpolarized leads. Further increase in V_g causes a maximum of $m_{\rm QD}$ to appear, followed by $m_{\rm QD}=0$, when $\epsilon_d^{\rm II}$ is in resonance with ϵ_F for $V_g=U$, and then minimum. Note that the $m_{\rm QD}$ maximum is weakened, as compared to one at $V_g \sim 0$, and the minimum is enhanced. It is due to electron interactions: the spectral weight of the second Hubbard level $\epsilon_\sigma^{\rm II}$ is $\sim \langle n_{\bar{\sigma}} \rangle$ [see Eq. (4)]. It also causes the dot magnetic moment to remain negative for large positive V_g (compare to $m_{\rm QD} > 0$ for large negative V_g).

An increase in the α symmetry of the dot-lead coupling causes a gradual decrease in the dot magnetic moment for AP configuration [panel (b) of Fig. 7]. For symmetric case of $\alpha = 1$, the magnetic moment is zero in whole range of gate voltages, as has been pointed out in the discussion of TMR maximum at zero bias. For $\alpha < 1$ the $m_{\rm QD}=0$ line collapses into one V_g point at which the TMR maximum appears.

(ii) The second field is an effective magnetic field, $H_{\rm eff}$, produced by magnetized electrodes. Its value is not dependent on gate voltage but rather on the relative leads polarizations. While TMR measurement is performed, the external magnetic field is applied to the system, which changes relative leads polarizations. Due to the intentionally different shape anisotropy of the left and right leads, the magnetization of each lead responds differently to the external field. It enables antiparallel lead polarization for small field and parallel configuration for higher field. The dot itself is in turn subjected to an effective magnetic field produced by the magnetic electrodes nearby. This field is the largest for parallel configuration.

For InAs quantum dots gyromagnetic ratio is negative, $g < 0$ (Ref. 27); thus the spin moments of $\epsilon_{d\uparrow}$ and $\epsilon_{d\downarrow}$ point in the same direction as the corresponding magnetic moments. The dot level subjected to the field $H_{\rm eff}$ produced by the polarized leads (of direction opposite to the leads spin polarization) is Zeeman split: $\epsilon_{d\downarrow} = \epsilon_d - \Delta$ and $\epsilon_{d\uparrow} = \epsilon_d + \Delta$, $\Delta = |g \mu_B H_{\rm eff}/2|$. The Zeeman energy splitting for $|g| = 3.8$ (Ref. 13) gives $2\Delta = 0.22$ meV/T ($=0.015U$ per tesla). We considered the influence of $H_{\rm eff}$ on the TMR features, assuming $H_{\rm eff}^{\rm P}$ of the order of $\pm 0.1T$, taken from experiments.[10,11] For antiparallel configuration the cancellation of the fields originating from the leads has been assumed $H_{\rm eff}^{\rm AP}=0$. We have found that the possible Zeeman splitting of the dot level has negligible effect on TMR in this field range.

VI. CONCLUSIONS

We have discussed the TMR anomalies encountered for the quantum dot coupled to spin-polarized leads in the regime of Coulomb blockade. We have shown that there are two kinds of such anomalies. One kind has the single-particle origin and can be interpreted in the frame of noninteracting electron model. The second kind of anomalies is caused by electron interactions. The TMR minima (and its sign change) of single-particle origin appear at the conductance resonances for asymmetric dot-lead coupling. They are robust to the temperature increase and gradually transform into local maxima when the symmetry of the dot-lead coupling increases. The anomalies associated with electron interactions appear at Coulomb blockade in between conductance resonances. The TMR maximum at Coulomb blockade, far exceeding 100%, is of this origin. It appears when, in antiparallel configuration, both the current and the dot occupancy are spin unpolarized. This maximum survives at typical temperatures of experiment. We also predict the TMR sign change at Coulomb blockade. It appears due to the rapid polarization switching of the current in AP configuration and the enhancement of the conductance in one of the AP spin channels by the dot-lead coupling asymmetry. It is very sensitive to the increase in temperature and depends on the initial polarization of the current coming from the leads. We have shown that the nature of the discussed anomalies can be experimentally resolved by the change in the dot-lead coupling asymmetry and/or temperature. Finally, we have analyzed the dot polarization, as induced by the coupling to the polarized leads, and shown that it also depends on electron interactions present inside the dot. The estimated Zeeman field splitting, produced by the leads, has negligible effect on TMR for experimental range of the fields.

ACKNOWLEDGMENTS

The work is supported by the European Science Foundation EUROCORES Programme FoNE by funds from the Ministry of Science and Higher Education and EC 6FP (Contract No. ERAS-CT-2003–980409).

---

*piotrs@ifmpan.poznan.pl

[1] J. S. Moodera, L. R. Kinder, T. M. Wong, and R. Meservey, Phys. Rev. Lett. **74**, 3273 (1995).
[2] M. Jullière, Phys. Lett. **54A**, 225 (1975).
[3] E. Y. Tsymbal, in *Handbook of Magnetism and Advanced Magnetic Materials, Vol. 5: Spintronics and Magnetoelectronis*, edited by H. Kronmüller and S. Parkin (Wiley, New York, 2007).
[4] I. Žutić, J. Fabian, and S. Das Sarma, Rev. Mod. Phys. **76**, 323 (2004).
[5] M. Y. Zhuravlev, E. Y. Tsymbal, and A. V. Vedyayev, Phys. Rev. Lett. **94**, 026806 (2005).
[6] Y. Ren, L. Zheng-zhong, X. Ming-wen, and A. Hu, Phys. Rev. B **75**, 054420 (2007).
[7] L. Jacak, P. Hawrylak, and A. Wójs, *Quantum Dots* (Springer-Verlag, New York, 1998).
[8] L. P. Kouwenhoven, C. M. Marcus, P. L. McEuen, S. Tarucha, R. M. Westervelt, and N. S. Wingreen, *Electron Transport in Quantum Dots* (Kluwer Academic Publishers, Dordrecht, 1997), Series E Vol. 345, p. 105.
[9] D. Goldhaber-Gordon, H. Shtrikman, D. Mahalu, D. Abush-

Magder, U. Meirav, and M. A. Kastner, Nature (London) **391**, 156 (1998).

[10] K. Hamaya, S. Masubuchi, M. Kawamura, T. Machida, M. Jung, K. Shibata, K. Hirakawa, T. Taniyama, S. Ishida, and Y. Arakawa, Appl. Phys. Lett. **90**, 053108 (2007).

[11] K. Hamaya, M. Kitabatake, K. Shibata, M. Jung, M. Kawamura, K. Hirakawa, T. Machida, T. Taniyama, S. Ishida, and Y. Arakawa, Appl. Phys. Lett. **91**, 022107 (2007).

[12] K. Hamaya, M. Kitabatake, K. Shibata, M. Jung, M. Kawamura, S. Ishida, T. Taniyama, K. Hirakawa, Y. Arakawa and T. Machida, Phys. Rev. B **77**, 081302(R) (2008).

[13] Y. Igarashi, M. Jung, M. Yamamoto, A. Oiwa, T. Machida, K. Hirakawa and S. Tarucha, Phys. Rev. B **76**, 081303(R) (2007).

[14] S. Sahoo, T. Kontos, J. Furrer, C. Hoffmann, M. Gräber, A. Cottet, and C. Schönenberger, Nat. Phys. **1**, 99 (2005).

[15] A. Jensen, J. R. Hauptmann, J. Nygard, and P. E. Lindelof, Phys. Rev. B **72**, 035419 (2005).

[16] J. Barnas and A. Fert, Phys. Rev. Lett. **80**, 1058 (1998).

[17] P. Zhang, Q.-K. Xue, Y. P. Wang, and X. C. Xie, Phys. Rev. Lett. **89**, 286803 (2002).

[18] M.-S. Choi, D. Sánchez, and R. López, Phys. Rev. Lett. **92**, 056601 (2004).

[19] P. Stefański, Phys. Rev. B **77**, 125331 (2008).

[20] P. W. Anderson, Phys. Rev. **124**, 41 (1961).

[21] A. C. Hewson, Phys. Rev. **144**, 420 (1966).

[22] H. Haug and A.-P. Jauho, *Quantum Kinetics in Transport and Optics of Semiconductors* (Springer, Berlin, 1996); A.-P. Jauho, N. S. Wingreen, and Y. Meir, Phys. Rev. B **50**, 5528 (1994).

[23] The absolute value of correlator $C=\langle n_\sigma^\beta n_{\bar{\sigma}}^\beta\rangle - \langle n_\sigma^\beta\rangle\langle n_{\bar{\sigma}}^\beta\rangle$ has the largest value in the region of $\epsilon_d \sim -U/2$.

[24] S. Takahashi and S. Maekawa, Phys. Rev. Lett. **80**, 1758 (1998).

[25] L. F. Schelp, A. Fert, F. Fettar, P. Holody, S. F. Lee, J. L. Maurice, F. Petroff, and A. Vaures, Phys. Rev. B **56**, R5747 (1997).

[26] K. Yakushiji, S. Mitani, K. Takanashi, S. Takahashi, S. Maekawa, H. Imamura, and H. Fujimori, Appl. Phys. Lett. **78**, 515 (2001).

[27] M. F. Doty, M. Scheibner, A. S. Bracker, I. V. Ponomarev, T. L. Reinecke, and D. Gammon, Phys. Rev. B **78**, 115316 (2008).